F. ABDO* , A. FAVE*, M. LEMITI*, A. LAUGIER*, C. BERNARD**, A. PISH**

STUDY OF Sn-Cu-Al-Si PHASE DIAGRAMS FOR GROWTH OF SILICON THIN FILM BY LIQUID PHASE EPITAXY

BADANIE DIAGRAMÓW FAZOWYCH Sn-Cu-Al-Si W CELU OKREŚLENIA WZROSTU CIENKIEJ WARSTWY KRZEMU METODĄ EPITAKSJI Z FAZY CIEKŁEJ

Silicon thin films are attracting considerable interest as a possible means of achieving low cost solar cells. In order to absorb 90% of the solar spectra, the thickness of such film has to be 30 μm. In this paper we compared LPE growth using pure Sn melt or Sn-Cu alloys at temperature below 800°C and their potential for photovoltaic applications. From Sn melt, one can achieved maximum thickness of 15 μm. Thickness is limited by the low solubility of Si in the melt. However from Sn-Cu solutions, when composition is carefully chosen, solubility is more important. Then thickness as much as 30 μm has been obtained. Furthermore, we described experimental technique allowing in situ removal of silicon native oxide prior to the growth.

Keywords: Liquid Phase Epitaxy, Cu-Al-Sn phase diagrams, Si epitaxial growth, low temperature

Krzemowe cienkie warstwy są wzbudzają znaczne zainteresowanie jako możliwość uzyskania tanich ogniw słonecznych. Aby zaabsorbować 90% widma słonecznego, grubość takiej warstwy musi mieć 30 μm. W pracy porównujemy wzrost LPR stosując czystą ciecz Sn lub stopy Sn-Cu w temperaturze poniżej 800°C i ich potencjalne zastosowanie w fotowoltaice. Stosując ciecz Sn można uzyskać maksymalną grubość 15 μm. Grubość jest ograniczona przez niską rozpuszczalność Si w cieczy. Jednak dla roztworów Sn-Cu, gdy skład jest dokładnie określony, rozpuszczalność jest bardziej istotna. W tym przypadku uzyskano grubość dochodzącą do 30 μm. Ponadto opisujemy doświadczalne techniki umożliwiające usuwanie "in situ" rodzimego tlenku krzemu poprzedzające wzrost.

1. Introduction

Development of photovoltaic modules in the past years and recent increase of silicon raw material cost give a certain interest to Liquid Phase Epitaxy technique for thin film silicon solar cell applications. It is a thin film growth technique that presents some interest regarding its low cost. Moreover, contrary to CVD, LPE permits single crystal growth even at low temperature.

This paper describes liquid phase epitaxy LPE method that has been developed to grow 15–30 μm thick monocrystalline silicon layers below 800°C. LPE has been widely studied at high temperature using solvents like tin or indium but only few works deal with low temperature LPE. Also low growth temperature is important to minimise the effect of thermal expansion mismatch (when using foreign substrate with seed layer) and to improve the rejection of impurities atoms from the growing film into the melt. Main difficulties, com-

pared to conventional LPE at 900–1000°C, are the low solubility of silicon in usual solvent and the presence of native silicon oxide that cannot be removed under H_2 flow.

In this paper we will present various results obtained from pure Sn melt and Sn-Cu based alloys. We will compare the respective growth rate that can be achieve and discuss about the development of such technique from experimental results and from calculated phase diagram.

2. Experiments with tin melt

All experiments were carried out in a horizontal graphite sliding boat at atmospheric pressure under hydrogen or argon gas flow. CZ-Si substrates are p+ type ($\rho < 0.01\Omega$.cm) with a (111) oriented and a size of 1×1 cm^2. In this study several solvents were used: Sn (5N), In (6N), Cu (5N) and Al (6N).

* LPM, UMR - CNRS 5511, INSA-LYON, BAT BLAISE PASCAL, 7 AVENUE JEAN CAPELLE, 69621 VILLEURBANNE, FRANCE
** LTPCM, UMR 5614, INPG-E.N.S.E.E.G, 1130 RUE DE LA PISCINE, BP 75, 38402 ST MARTIN D'HERES, FRANCE

534

Prior to epitaxy, one has to remove the native silicon oxide from the substrate surface. At temperature above 900°C, it is ensured by gaseous H_2. However, the use of reducing metal like aluminium is necessary for our experimental temperature. Addition of a few amount of Al in the melt is sufficient to etch silicon oxide, but it then leads to a too high increment of doping level of the grown Si epilayer. So we developed a technique using two different melts, one to remove native oxide, the other one to grow the active layer.

First melt is an alloy with low amount of Al, but enough to reduce SiO_2. The melts were saturated with silicon at 795°C. The key point is the realisation of a melt-back at 800°C. It consists in introducing the substrate under this melt at a higher temperature than the saturation temperature which will enhance the dissolution of the native silicon oxide of the substrate. Afterwards the substrate was moved under the second melt. The temperature was decreased at a rate of 0.5°C/min until the final temperature during 2 or 3 hours. This process of cooling down causes supersaturation of the melt with resultant precipitation of the silicon on the substrate to form the epitaxial layer. Separation of cleaning and growth step avoids the diffusion of Al in the whole active epilayer.

With using Sn melt, this technique leads to smooth and homogeneous Si layer with p+/p structure (10–15 μm Ga doped active layer, 2 μm Al highly doped interface layer). Thickness of the layers is about 10–15 μm after 3hours of growth under hydrogen or argon flow. Note that presence of Ga doesn't affect significantly growth rate and solubility of Si in the melt. From such p/p+ structure grown on a highly doped Si substrate (so this substrate is "inactive" regarding gen-

eration of carriers) we fabricated solar cells using phosphorus diffusion (at 900°C during 20 minutes) to get the n+/p junction. Metallic contacts of Al on the rear p+ substrate side and of Ti-Pd-Ag on the front side are evaporated then annealed at 400°C during 30 minutes under H_2. To minimize surface reflectivity, an hydrogenated silicon nitride SiN_x: H film is deposited by Low Frequency Plasma Enhanced Chemical Vapour Deposition (LF-PECVD). Photovoltaic results showed that short circuit current is only 17 mA/cm^2 (for industrial Si solar cell, it should be around 35 mA/cm^2). In fact absorption of photons is decreasing for wavelength higher than 600 nm mainly because film thickness is too small [1].

3. Binary and ternary systems

Study of the Si-Sn binary phase diagram (figure 1) [2] shows the low solubility of silicon in tin (0.63 at.% at 800°C). It is known that the growth rate of silicon, in the 700-900°C range, decreases with decreasing solubility of silicon. Several concepts have been proposed in order to increase the solubility of silicon like the use of ternary and quaternary alloys. We classified the metals in two categories.

Type I metals (Bi, In, Sn, Pb) have low melting point. They present a pseudo eutectic with Si but with only less than 1at% Si at this point. Type II metals (Al, Au, Ag, Cu) all form an eutectic with silicon with more than 10at% Si at the eutectic point. Al and Ga are suitable regarding temperature and growth rate. However, resulted layers present heavy doping and are useless for electronic or photovoltaic applications [3]. Copper's eutectic with silicon is encountered at too high temperature (T>800°C).
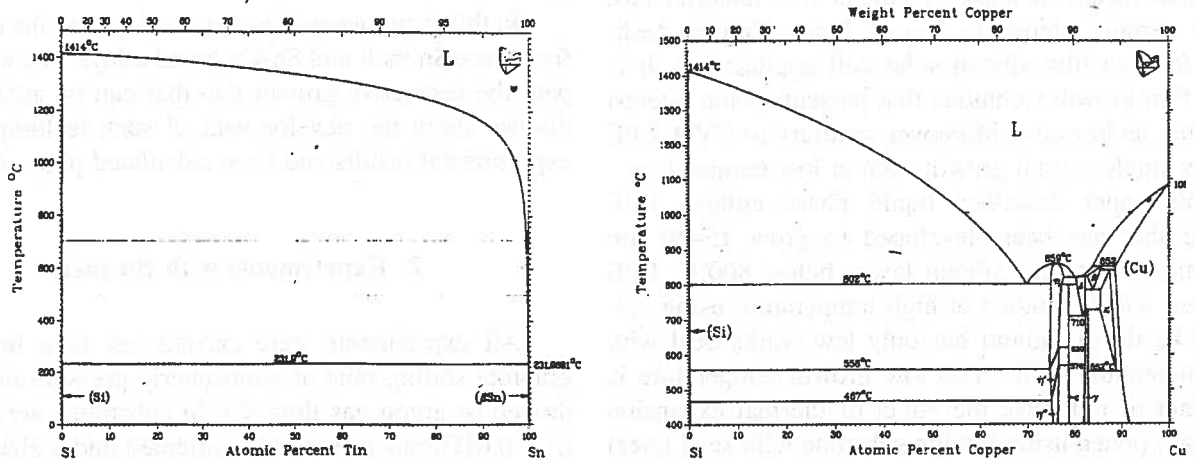

Fig. 1. Binary systems Si-Sn and Si-Cu

To increase solubility and decrease growth temperature, it is necessary to combine a type I and a type II metals.

Among type I metals, we selected tin for theses reasons:

1) low growth temperature
2) low vapour pressure
3) low toxicity
4) electrical inactivity with silicon.

But, main disadvantage is, as we mentioned, the low solubility of silicon. At 700°C, growth rate cannot be higher than 0.05 μm/min. However, when it is used with suitable other metallic elements, one can improve the solubility.

Copper is an attractive candidate for metal solution growth of Si thin layers among type II metals for theses reasons:

1) high solubility of silicon
2) low solid solubility of Cu in Si (when low cooling rate is applied, incorporation of Cu is minimized [4])
3) minimal effect on doping level and resistivity of the layer: Cu is not a doping element.

The Cu-Si phase diagram [5] is complex on the copper rich side, but it offers a wide temperature range for solution growth at compositions ~30at% Si at the eutectic temperature of 802°C (figure1). It is possible to grow Si layer from pure Cu melt but only at high temperature (> 802°C). Incorporation of Cu in the Si epitaxial layer is minimized when cooling rate is lower than 0.5°C/min and does not affect the quality of junction [4]. To form a suitable melt for LPE below 800°C, an alloy with a type I metal component is required.
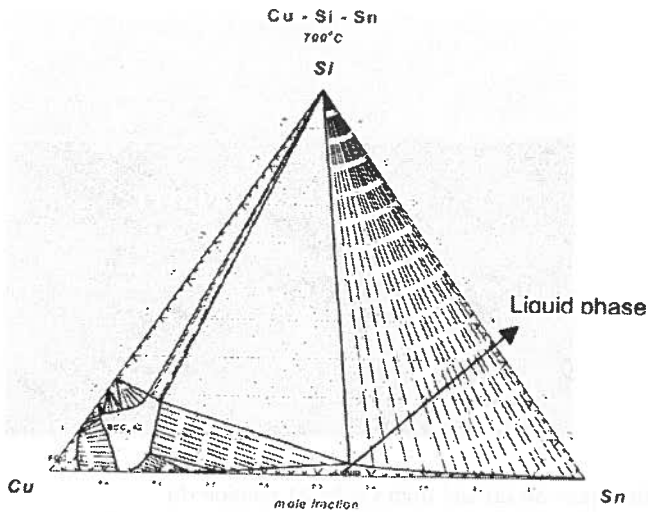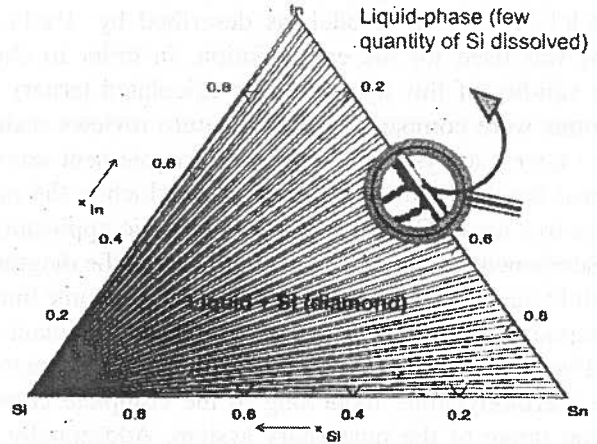

Fig. 3. Ternary system In-Si-Sn at 727°C, P 1bar

Tin based ternary alloy Cu-Sn-Si is illustrated on figure 2 and is compared to the ternary alloy In-Sn-Si (figure 3). Regarding the ternary system In-Sn-Si, whatever is the composition, only a few quantity of Si can be dissolved into the liquid phase: such ternary system which contains two type I metals (Sn and In) does not demonstrate low temperature increasing of Si solubility. Moreover we didn't notice any improvement of growth kinetics when changing composition, compared to pure Sn melt [6]. However, in the ternary system Cu-Sn-Si, liquid phase region is much larger. As we explained previously, addition of aluminium in the melt is required to etch the native silicon oxide. For this reason, a thermodynamic equilibrium calculation for the quaternary alloy Cu-Sn-Al-Si was also studied.

4. Thermodynamic equilibrium calculations

The phase equilibria in Cu-Si-Sn and Al-Cu-Si-Sn were calculated using optimized Gibbs energy datasets for all phases and compounds obtained by the Calphad method. The data for all binary systems were taken from the litterature : Al-Cu [7], Al-Si [8], Al-Sn [9], Cu-Si [10], Cu-Sn [11] and Si-Sn[12]. The liquid phase was modelled as a disordered solution phase using R e d l i c h - K i s t e r polynomials to describe the excess G i b b s energy of mixing. The Factsage software package [13] was used for the phase diagram calculations. This software allows different extrapolation methods to higher order systems. This is particularly important in ternary systems in which one of the three binaries behaves chemically different than the two others. This is the case in the Cu-Si-Sn or Al-Cu-Si ternaries in which the Si-Sn or Al-Si liquid phase is almost ideal (Al-Si) or shows a tendency of demixing (Si-Sn) whereas Al-Cu, Cu-Si and Cu-Sn have all negative ex-

Fig. 2. Ternary system Cu-Si-Sn at 700°C, P 1bar

cess G i b b s energies. Therefore, the unsymmetrical K o h l e r / T o o p model, as described by P e l t o n [14] was used for the extrapolation. In order to check the validity of this approach, the calculated ternary diagrams were compared to the literature reviews such as T e r n a r y alloys [15]. A reasonable agreement was obtained for the liquid – (Si) equilibria which is the main objective for LPE growth and photovoltaic applications. Discrepancies occur in some other parts of the diagrams, mainly due to omitted ternary solubilities in some binary compounds. However, because this was not the main objective of this study, no effort was undertaken to improve the thermodynamic modelling in the complete composition range of the quaternary system. Additionally, no ternary interaction parameters were introduced, neither for the liquid phase nor for the solid solutions.

5. Experimental results and discussion for Sn-Cu melts

For Cu-Sn melt, the study of quaternary alloy Cu-Si-Sn-Al (10%Wt Al) shows a liquid phase in the Sn rich side at 800°C (figure 4), so it can be used as melt1 with this composition. At 800°C, Si solubility increases up to 2 Wt% with this alloy (with pure Sn melt, Si solubility is only 0.16 Wt% at same temperature). Experimental results obtained with this alloy at 800°C lead to a growth rate of 0.25 μm/min compared to 0.08 μm/min with Sn solvent. Figure 5 shows the cross section of Si layer grown at 800°C from Cu_{10}-Sn_{78}-Si_2-Al_{10}. Thickness is as much as 30 μm after cooling down from 800 to 770°C, meanwhile when using pure Sn solvent, maximum thickness obtained is 15 μm after cooling down from 800 to 710°C.
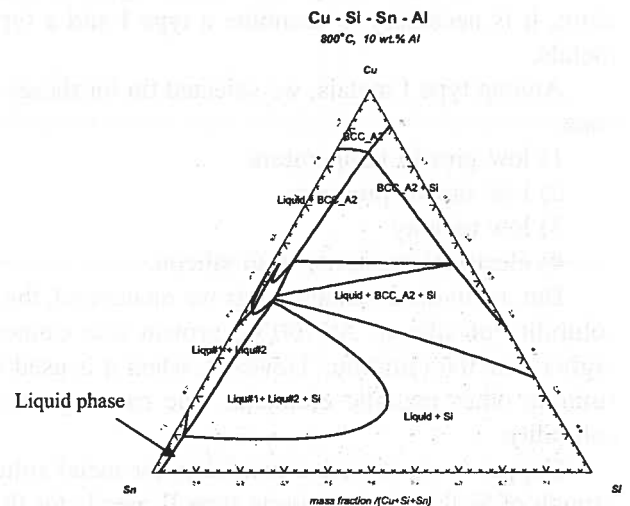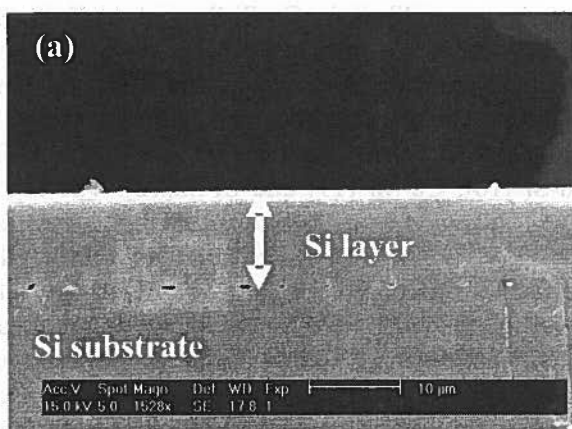

Fig. 4. Quaternary system Cu-Si-Sn-Al (10%wt Al) at 800°C, P:1bar

This phase diagram is quite complex and is changing with temperature. For this reason, a complete knowledge of phase evolution between starting and ending temperature is necessary. We calculated the phase proportion evolution with temperature to ensure there is only one liquid phase in equilibrium with solid Si. As an example, figure 6 shows the phase proportion variation wit temperature of the following melt: $Cu_{0.25}Al_{0.14}Sn_{0.5}Si_{0.11}$. It can be used from 900°C until 810°C for silicon growth and it presents high growth rate. However, from 810°C, as one can see on the figure, a second liquid phase appears and it is not miscible with the first one. Therefore during cooling down below 810°C, this phase leads to the formation of crystalline defects in the layer (see insert of figure 6).
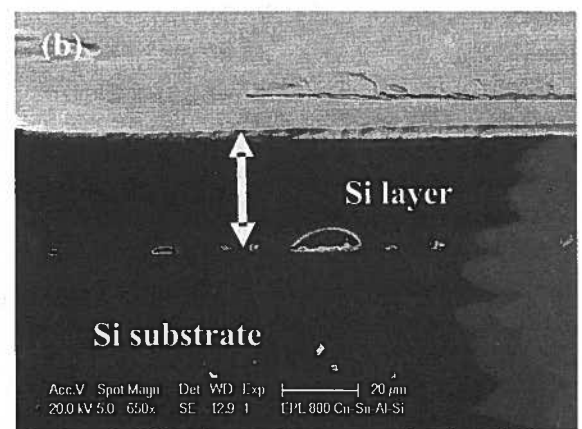

Fig. 5. SEM micrograph of Si layers grown at 800°C from pure Sn (a) and from Cu-Sn-Al solution (b)
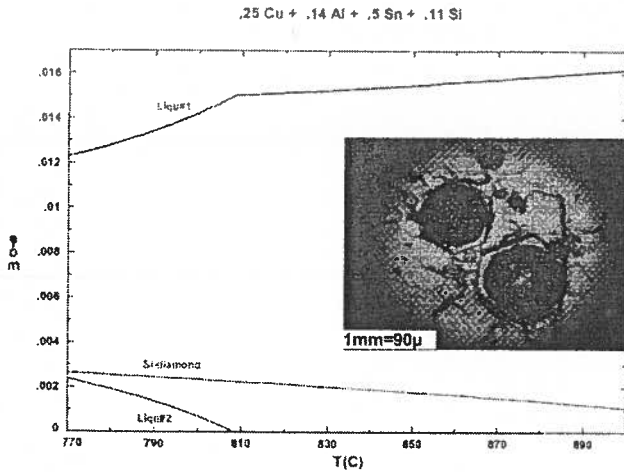
.25 Cu + .14 Al + .5 Sn + .11 Si

Fig. 6. Phase proportion variations with temperature in the Cu-Al-Sn-Si

6. Conclusion

Low temperature liquid phase epitaxial growth of Si was investigated from Sn and Cu-Sn solutions using ternary and quaternary phase diagram studies. We described a two melts technique allowing in situ removal of silicon oxide. We compared maximum film thickness that can be obtained in the 700-800°C range with these solvents. Maximum growth rate for Sn melt is only 0,08 μm/min. But for Sn-Cu alloys, growth rate is 0.25 μm/min and more, and lead to flat and homogeneous thin films. Therefore, the growth of 30 μm thick film in a reasonable time can has been demonstrated. With such thickness, Si film can absorb 90% of the solar spectra and solar cell can be fabricated.

REFERENCES

[1] F. Abdo, A. Fave et al., Proceeding of EXMATEC'06 conference, Cadiz (Spain); 14-17 May 2006.
[2] J. L. Murray, Binary Alloys Phase Diagrams, 2049 (1983).
[3] Soo Hong Lee, Martin A. Green, J. Electronic materials, 20, 8, 635-641 (1991).
[4] T. H. Wang et al., 25th Photovoltaic specialist Conference, Washington, D.C, 1996, pp 689-692.
[5] J. L. Murray, Binary Alloys Phase Diagrams, 960 (1983).
[6] F. Abdou, A. Fave, M. Lemiti, A. Laugier, C. Bernard, A. Pisch, IEEE-31st photovoltaic specialist conference, Orlando, 2005.
[7] N. Saunders in: I. Ansara, A. T. Dinsdale, M. H. Rand (eds.): COST 507, Thermochemical database for light metal alloys 2, EUR18499 28-33 (1998).
[8] H. Feufel, T. Gödecke, H. L. Lukas, F. Sommer, J. Alloys Comp. 247 31-42 (1997).
[9] S. G. Fries, H. L. Lukas in: I. Ansara, A. T. Dinsdale, M. H. Rand (eds.): COST 507, Thermochemical database for light metal alloys 2, EUR18499 81-82 (1998).
[10] M. H. G. Jacobs in: I. Ansara, A. T. Dinsdale, M. H. Rand (eds.): COST 507, Thermochemical database for light metal alloys 2, EUR18499 178-181 (1998).
[11] J.-H. Shim, C.-S. Oh, B.-J. Lee, D. N. Lee, Z. Metallkd. 87, 205-212 (1996).
[12] M. H. G. Jacobs, Ph. Spencer, Calphad 20, 89-91 (1996).
[13] C. W. Bale, P. Chartrand, S. A. Degterov, G. Eriksson, K. Hack, R. Ben Mahfoud, J. Melançon, A. D. Pelton, S. Petersen, Calphad 26(2), 189-228 (2002).
[14] A. D. Pelton, Calphad 25(2), 319-328 (2001).
[15] G. Effenberg, Ternary Alloys, VCH Verlag, Weinheim (Germany).